

Soliton-effect compression of supercontinuum to few-cycle durations in photonic nanowires

Mark A. Foster and Alexander L. Gaeta

School of Applied and Engineering Physics, Cornell University, Ithaca, NY 14853

maf42@cornell.edu, alg3@cornell.edu

Qiang Cao and Rick Trebino

School of Physics, Georgia Institute of Technology, Atlanta, GA 30332-0430

Abstract: By exploiting the broad region of anomalous group-velocity dispersion (GVD) and the large effective nonlinearity of photonic nanowires, we demonstrate soliton-effect self-compression of 70-fs pulses down to 6.8 fs. Under suitable conditions, simulations predict that self-compression down to single-cycle duration is possible.

© 2005 Optical Society of America

OCIS codes: (320.5520) Pulse compression; (320.2250) Femtosecond phenomena; (190.5530) Pulse propagation and solitons; (320.7140) Ultrafast processes in fibers

References and links

1. L. Xu, C. Spielmann, A. Poppe, T. Brabec, F. Krausz, T. W. Hansch, "Route to phase control of ultrashort light pulses," *Opt. Lett.* **21**, 2008-2010 (1996).
2. H. R. Telle, G. Steinmeyer, A. E. Dunlop, J. Stenger, D. H. Sutter, U. Keller, "Carrier-envelope offset phase control: A novel concept for absolute optical frequency measurement and ultrashort pulse generation," *Appl. Phys. B* **69**, 327-332 (1999).
3. M. Ivanov, P. B. Corkum, T. Zuo, A. Bandrauk, "Routes to Control of Intense-Field Atomic Polarizability," *Phys. Rev. Lett.* **74**, 2933-2936 (1995).
4. I. P. Christov, M. M. Murnane, H. C. Kapteyn, "High-harmonic generation of attosecond pulses in the 'single-cycle' regime," *Phys. Rev. Lett.* **78**, 1251-1254 (1997).
5. I. P. Christov, "Phase-dependent loss due to nonadiabatic ionization by sub-10-fs pulses," *Opt. Lett.* **24**, 1425-1427 (1999).
6. S. Chelkowski, A. D. Bandrauk, "Sensitivity of spatial photoelectron distributions to the absolute phase of an ultrashort intense laser pulse," *Phys. Rev. A* **65**, 061802 (2002).
7. L. Xu, C. Spielmann, F. Krausz, R. Szipocs, "Ultrabroadband ring oscillator for sub-10-fs pulse generation," *Opt. Lett.* **21**, 1259-1261 (1996).
8. U. Morgner, F. Kartner, S. H. Cho, E. Chen, H. A. Haus, J. G. Fujimoto, E. P. Ippen, V. Scheuer, G. Angelow, T. Tschudi, "Sub-two-cycle pulses from a Kerr-lens mode-locked Ti:sapphire laser," *Opt. Lett.* **24**, 411-413 (1999).
9. D. H. Sutter, G. Steinmeyer, L. Gallmann, N. Matuschek, F. Morier-Genoud, U. Keller, V. Scheuer, G. Angelow, T. Tschudi, "Semiconductor saturable-absorber mirror-assisted Kerr-lens mode-locked Ti : sapphire laser producing pulses in the two-cycle regime," *Opt. Lett.* **24**, 631-633 (1999).
10. A. Baltuska, Z. Wei, M. S. Pshenichnikov, D. A. Wiersma, "Optical pulse compression to 5 fs at a 1-MHz repetition rate," *Opt. Lett.* **22**, 102-104 (1997).
11. M. Nisoli, S. DeSilvestri, O. Svelto, R. Szipocs, K. Ferencz, C. Spielmann, S. Sartania, F. Krausz, "Compression of high-energy laser pulses below 5 fs," *Opt. Lett.* **22**, 522-524 (1997).
12. N. Karasawa, L. M. Li, A. Suguro, H. Shigekawa, R. Morita, M. Yamashita, "Optical pulse compression to 5.0 fs by use of only a spatial light modulator for phase compensation," *J. Opt. Soc. Am. B* **18**, 1742-1746 (2001).

13. B. Schenkel, J. Biegert, U. Keller, C. Vozzi, M. Nisoli, G. Sansone, S. Stagira, S. De Silvestri, O. Svelto, "Generation of 3.8-fs pulses from adaptive compression of a cascaded hollow fiber supercontinuum," *Opt. Lett.* **28**, 1987-1989 (2003).
14. K. Yamane, Z. Zhang, K. Oka, R. Morita, M. Yamashita, A. Suguro, "Optical pulse compression to 3.4fs in the monocycle region by feedback phase compensation," *Opt. Lett.* **28**, 2258-2260 (2003).
15. C.P. Hauri, W. Kornelis, F.W. Helbing, A. Heinrich, A. Couairon, A. Mysyrowicz, J. Biegert, and U. Keller, "Generation of intense, carrier-envelope phase-locked few-cycle laser pulses through filamentation," *Appl. Phys. B* **79**, 673-677 (2004).
16. B. Schenkel, R. Paschotta, U. Keller, "Pulse compression with supercontinuum generation in microstructure fibers," *J. Opt. Soc. Am. B* **22**, 687-693 (2005).
17. G. P. Agrawal, *Nonlinear Fiber Optics* (Academic Press, 1989).
18. D. Akimov, M. Schmitt, R. Maksimenka, K. Dukel'skii, Y. Kondrat'ev, A. Khokhlov, V. Shevandin, W. Kiefer, and A. M. Zheltikov, "Supercontinuum generation in a multiple-submicron-core microstructure fiber: toward limiting waveguide enhancement of nonlinear-optical processes," *Appl. Phys. B* **77**, 299-305 (2003).
19. L. M. Tong, R. R. Gattass, J. B. Ashcom, S. L. He, J. Y. Lou, M. Y. Shen, I. Maxwell, and E. Mazur, "Subwavelength-diameter silica wires for low-loss optical wave guiding," *Nature* **426**, 816-819 (2003).
20. A. M. Zheltikov, "The physical limit for the waveguide enhancement of nonlinear-optical processes," *Opt. Spectrosc.* **95**, 410-415 (2003).
21. L. M. Tong, J. Y. Lou, and E. Mazur, "Single-mode properties of sub-wavelength-diameter silica, and silicon wire waveguides," *Opt. Express* **12**, 1025-1035 (2004), <http://www.opticsexpress.org/abstract.cfm?URI=OPEX-12-6-1025>.
22. E. C. Mägi, P. Steinvurzel, and B. J. Eggleton, "Tapered photonic crystal fibers," *Opt. Express* **12**, 776-784 (2004), <http://www.opticsexpress.org/abstract.cfm?URI=OPEX-12-5-776>.
23. S. Leon-Saval, T. Birks, W. Wadsworth, P. St. J. Russell, M. Mason, "Supercontinuum generation in submicron fibre waveguides," *Opt. Express* **12**, 2864 (2004), <http://www.opticsexpress.org/abstract.cfm?URI=OPEX-12-13-2864>.
24. M. A. Foster, K. D. Moll, A. L. Gaeta, "Optimal waveguide dimensions for nonlinear interactions," *Opt. Express* **12**, 2880 (2004), <http://www.opticsexpress.org/abstract.cfm?URI=OPEX-12-13-2880>.
25. M. A. Foster, A. L. Gaeta, "Ultra-low threshold supercontinuum generation in sub-wavelength waveguides," *Opt. Express* **12**, 3137 (2004), <http://www.opticsexpress.org/abstract.cfm?URI=OPEX-12-14-3137>.
26. Y. Lize, E. C. Mägi, V. Ta'eed, J. Bolger, P. Steinvurzel, B. Eggleton, "Microstructured optical fiber photonic wires with subwavelength core diameter," *Opt. Express* **12**, 3209 (2004), <http://www.opticsexpress.org/abstract.cfm?URI=OPEX-12-14-32097>.
27. M. Law, D. J. Sirbully, J. C. Johnson, J. Goldberger, R. J. Saykally, P. Yang, "Nanoribbon waveguides for subwavelength photonics integration," *Science* **305**, 1269 (2004).
28. E. C. Mägi, H. C. Nguyen, B. J. Eggleton, "Air-hole collapse and mode transitions in microstructured fiber photonic wires," *Opt. Express* **13**, 453 (2005), <http://www.opticsexpress.org/abstract.cfm?URI=OPEX-13-2-453>.
29. M. A. Foster, J. M. Dudley, B. Kibler, Q. Cao, D. Lee, R. Trebino, and A. L. Gaeta, "Nonlinear pulse propagation and supercontinuum generation in photonic nanowires : experiment and simulation," *Appl. Phys. B*, **81**, 363-367 (2005).
30. T. Brabec, F. Krausz, "Nonlinear optical pulse propagation in the single-cycle regime," *Phys. Rev. Lett.* **78**, 3283 (1997).
31. A. L. Gaeta, "Nonlinear propagation and continuum generation in microstructured optical fibers," *Opt. Lett.* **27**, 924-926 (2002).
32. J. M. Dudley and S. Coen, "Coherence properties of supercontinuum spectra generated in photonic crystal and tapered optical fibers," *Opt. Lett.* **27**, 1180-1182 (2002).
33. J. M. Dudley, X. Gu, L. Xu, M. Kimmel, E. Zeek, P. O'Shea, R. Trebino, S. Coen, R. S. Windeler, "Cross-correlation frequency resolved optical gating analysis of broadband continuum generation in photonic crystal fiber: simulations and experiments," *Opt. Express* **10**, 1215 (2002), <http://www.opticsexpress.org/abstract.cfm?URI=OPEX-10-21-1215>.

1. Introduction

The generation of few-optical-cycle laser pulses has enabled investigations of a new regime of ultrafast optical interactions. Specifically, for few-cycle pulses the relative

position of the peak of the electric field and the peak of the electric field envelope, a parameter known as the carrier-envelope offset, becomes important in determining interactions with matter [1,2]. For example, attosecond-pulse generation, high-harmonic generation, photo-ionization, and multiphoton absorption are sensitive to this parameter [3–6]. Few-cycle pulses can be generated directly from laser oscillators using specifically designed dispersion compensation optics [7–9]. In addition, ultrafast pulses have been compressed to this regime by using a combination of self-phase-modulation-induced spectral broadening and post compression with passive and active components [10–16]. With these techniques, the ability to access the few-cycle regime has required either specially designed laser oscillators, amplified pulses with μJ -pulse energies, or spectral broadening with sophisticated post-compression schemes.

In this paper, we present a simple method to compress sub-nJ optical pulses with initial pulse widths as long as 100 fs down to few-cycle durations with no post compression. Specifically, we demonstrate theoretically and experimentally generation of few-cycle optical pulses using soliton-effect self-compression of octave-spanning super-continuum generated in photonic nanowires. The simplicity of this technique should allow for broader access to the few-optical-cycle regime and to the investigation of the unique properties of light-matter interactions with such pulses.

2. Soliton-effect compression

The combined action of anomalous group-velocity dispersion (GVD) and self phase modulation leads to the well known phenomenon of soliton-effect compression [17]. This phenomenon corresponds to the excitation of a higher-order soliton which undergoes cyclical temporal compression and spectral broadening followed by temporal spreading and spectral narrowing. By extracting from the appropriate cycle of this breathing mode, a temporally compressed pulse is generated. The optimal length z_{opt} at which to extract the compressed pulse can be predicted using the following empirical formula [17]:

$$\frac{z_{opt}}{L_D} = \frac{0.32}{N} + \frac{1.1}{N^2}, \quad (1)$$

where N is the soliton order defined as $N^2 = \frac{L_D}{L_{NL}}$, $L_D = \frac{T_{in}^2}{|\beta_2|}$ is the dispersion length, $L_{NL} = \frac{1}{\gamma P_0}$ is the nonlinear length, T_{in} is the duration of the input pulse, β_2 is the group velocity dispersion at the center wavelength, γ is the effective nonlinearity, and P_0 is the peak power of the input pulse. The efficiency of compression is characterized by the compression factor F_c and by the quality factor Q_c defined as [17]

$$F_c = \frac{T_{in}}{T_{comp}}, \quad (2)$$

$$Q_c = \frac{P_{comp}}{F_c}, \quad (3)$$

where T_{comp} is the duration of the compressed pulse, and P_{comp} is the peak power of the compressed pulse normalized to the input pulse. For efficient soliton-effect compression it is desirable to have small or slightly positive third-order dispersion, broad anomalous-GVD, and high nonlinearity [17].

3. Photonic nanowires

Recently, much research has focused on confining light in waveguiding structures that are on the order of and smaller than an optical wavelength [18–29]. Since these structures are typically sub-micron in size, such waveguides are termed photonic nanowires.

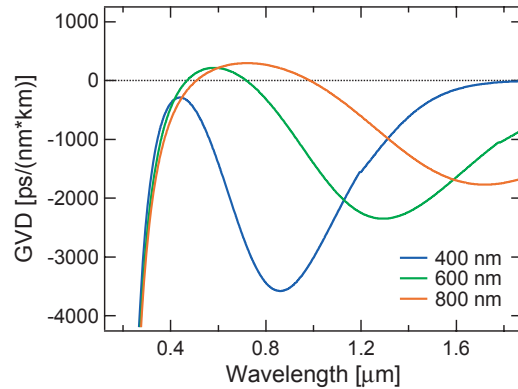


Fig. 1. Group-velocity dispersion of a circular glass nanowire in air for core diameters of 200 nm, 400 nm, 600 nm, and 800 nm.

Due to their tight optical confinement, photonic nanowires can exhibit large effective nonlinearities and a high sensitivity of the fundamental mode to the waveguide dimensions [20,21,24]. As is seen in Fig. 1, the large waveguide contribution to the dispersion can shift both zero-GVD points into the visible regime. Between these zero-GVD points lies a broad region of anomalous-GVD. By adjusting the size of the nanowire, this region of anomalous-GVD can be shifted throughout the visible and near-infrared. The large effective nonlinearities and tunable GVD of photonic nanowires have been shown to lead to efficient production of ultrafast nonlinear processes such as supercontinuum generation [23,25].

4. Simulation

Suitable conditions for soliton-effect compression are engineered by adjusting the nanowire dimensions. If the core diameter is made the same size or slightly larger than the pump wavelength, the broad region of anomalous-GVD is centered at this point and is accompanied by low third-order-dispersion at this wavelength. For a pump wavelength of 800-nm, the GVD profiles of 800-nm and 1- μ m-core diameter photonic

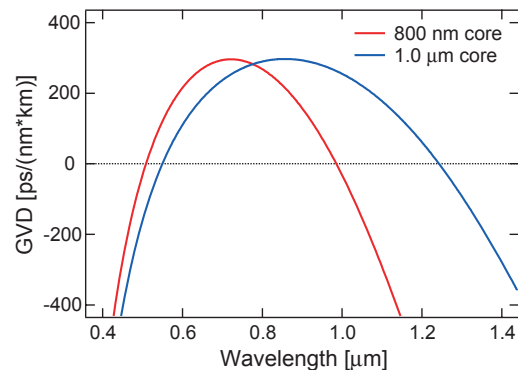


Fig. 2. Group-velocity dispersion of 800-nm and 1- μ m diameter glass rods in air appropriate for compression of an 800-nm center wavelength input pulse.

nanowires are shown in Fig. 2. Nanowires of these dimensions yield octave spanning regions of anomalous-GVD in the visible to near-infrared. The corresponding effective nonlinearities for 800-nm and 1- μm photonic nanowires, assuming a pump wavelength of 800 nm, are $502 (\text{W}\cdot\text{km})^{-1}$ and $370 (\text{W}\cdot\text{km})^{-1}$ respectively.

As an example, for an 800-nm core diameter nanowire, a 30-fs and 500-pJ pulse with an 800-nm center wavelength would correspond to the excitation of a soliton of order $N = 5.5$. Using Eq. (1), a $337\text{-}\mu\text{m}$ optimal nanowire length is predicted for this interaction. We simulate this interaction using the nonlinear-envelope equation and take into account the full-GVD profile [29–32]. The results of this simulation are shown in Fig. 3. The initially 30-fs pulse develops an octave-spanning spectrum and compresses down to a duration of 1.8 fs after a $650\text{-}\mu\text{m}$ propagation distance inside the nanowire. Although, the formation of a 1.8-fs feature corresponds to a duration of approximately a single-optical-cycle, we expect these results to be reasonably accurate since the nonlinear-envelope equation was shown to be valid down to this regime [30]. Most of the compression occurs near the end of the propagation distance as is shown by the behavior of the peak intensity in Fig. 4. This interaction corresponds to a compression factor F_c of 16.67 and a quality factor of compression Q_c of 0.48. While the simulated optimal length of $650\text{-}\mu\text{m}$ is the same order of magnitude as that predicted by Eq. (1), better agreement is most likely hampered due to the dispersion variation over the supercontinuum bandwidth. Furthermore, as is expected from the form of Eq. (1), the optimal length can be easily adjusted by varying the input pulse energy as seen in Fig. 4. This provides an important parameter to experimentally optimize the

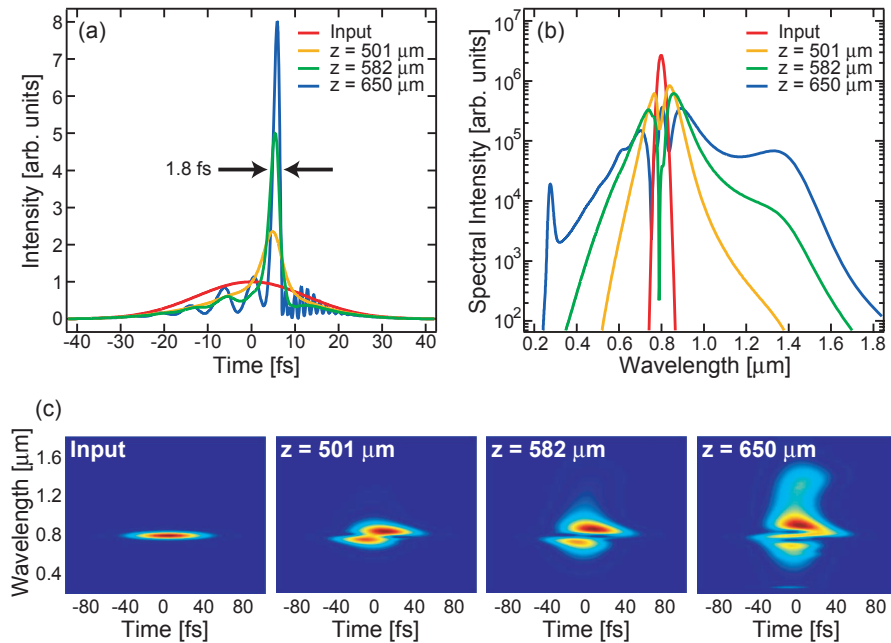


Fig. 3. Theoretically predicted (a) temporal and (b) spectral evolution of a 500-pJ and initially 30-fs Gaussian pulse undergoing soliton-effect compression in a 800-nm core diameter photonic nanowire at propagation distances of $501\text{ }\mu\text{m}$, $582\text{ }\mu\text{m}$, and $650\text{ }\mu\text{m}$. (c) Spectrogram representation of the pulse at each of the corresponding propagation distances. (1.54 MB)

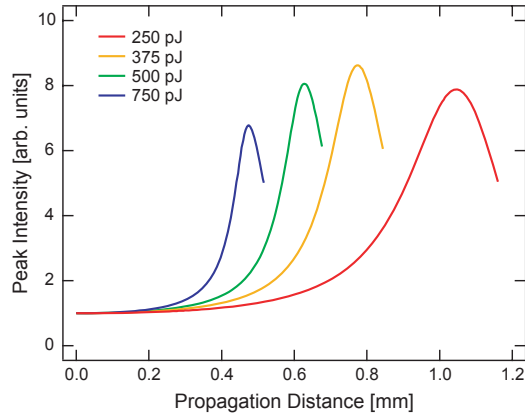


Fig. 4. Peak intensity of 250-pJ, 375-pJ, 500-pJ, and 750-pJ pulses as a function of propagation distance inside an 800-nm core diameter photonic nanowire.

generated compressed pulse for a specific nanowire length and input pulse duration. The ability to compress the pulse is indicative of the high coherence properties of the generated supercontinuum, which is distinguished from supercontinuum generated in longer lengths of fiber where spectral decoherence due to stimulated Raman scattering can occur [32].

5. Experiment

The method by which we fabricate waveguides of sub-micron core diameters was described previously [22, 23, 25]. This method consists of tapering the core diameter of a commercially available 2.3- μm -core microstructured fiber to sub-micron size. Special attention is paid to ensure the air-glass microstructured cladding remains intact during the tapering process. For this application, nanowire lengths on the order of 1-mm are necessary. We fabricate waveguides of these lengths by attaching the tapered microstructured fiber to a thin metal ridge and subsequently cleaving the nanowire to the desired length. Using this procedure waveguides of a desired core diameter and length were reproducibly fabricated. However, since the cleaving is done by hand, several waveguides were fabricated to ensure that one would couple light efficiently. An image of nanowires prepared with this method is shown in Fig. 5. The waveguiding is robust to this mounting procedure because the core is enclosed in the microstructured cladding and glass outer cladding [28]. In this way, the propagating light does not interact with the metal ridge or mounting adhesive. All of the experiments performed in this investigation made use of the pictured 980-nm core waveguide.

We generated supercontinuum in the 980-nm core diameter and 2-mm-long nanowire shown in Fig. 5 using a 30-fs input pulse from an 80-MHz Ti:Sapphire oscillator. The laser had a center wavelength of 800 nm and a 20x coupling objective with a 0.5 NA was used. An image of the supercontinuum generation is shown in Fig. 5. The measured spectral evolution as a function of average power before the coupling objective is shown in Fig. 6. Comparison with our simulations shows good agreement if a coupling efficiency of 8.33 percent is assumed. The coupling efficiency must be estimated since it is difficult to accurately measure this parameter experimentally due to the extremely short length of the nanowire.

We performed cross-correlation frequency resolved optical gating (XFROG) measure-

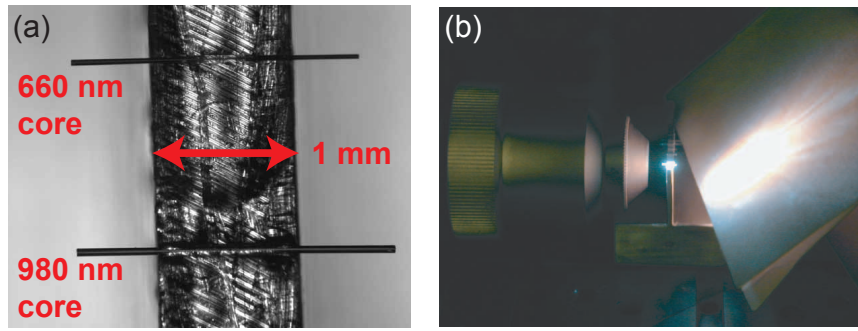


Fig. 5. (a) Optical microscope image of 660-nm and 980-nm core diameter photonic nanowires with 2-mm lengths mounted on a 1-mm metal ridge. (b) Supercontinuum generated in a 2-mm long photonic nanowire.

ments on the supercontinuum generated in the 980-nm core nanowire in order to characterize the generated pulse [33]. For this measurement, a 70-fs input pulse and a 40x coupling objective with a 0.65 NA were used. The average power from the 80-MHz Ti:Sapphire oscillator was 70 mW before the coupling objective. The longer pulse width was chosen since the longer dispersion length of this pulse allows greater compression in the fabricated 2-mm long nanowire as estimated by Eq. (1). Both the Ti:sapphire input pulse and XFROG reference pulse were characterized by using a GRENOUILLE device. For the XFROG measurement, a 40- μ m BBO crystal with angle dithering was used to guarantee phase matching of the broadband continuum. The compressed pulse is shown

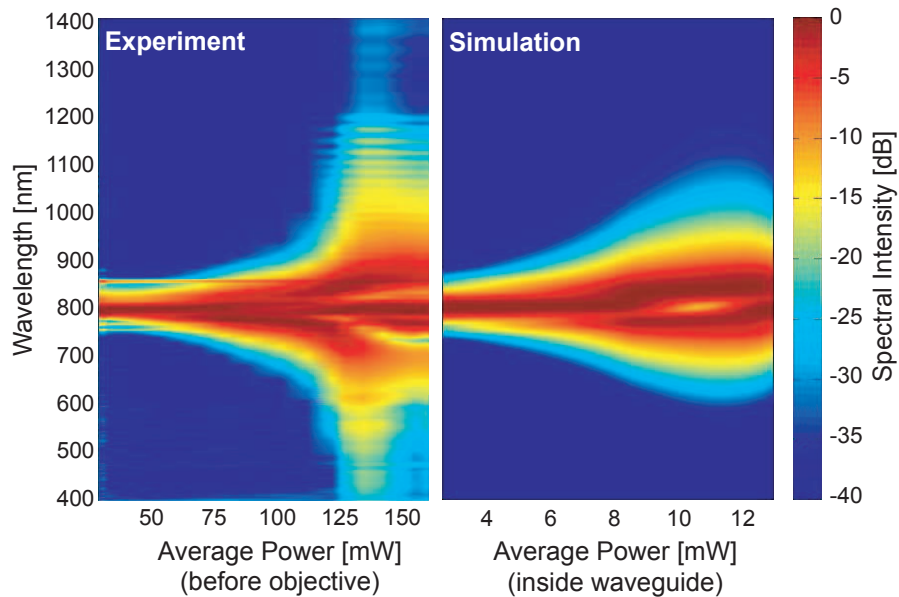


Fig. 6. Measured and simulated spectral evolution of supercontinuum generated as functions of average power of the mode-locked laser before the coupling objective (experiment) and inside the nanowire (simulation).

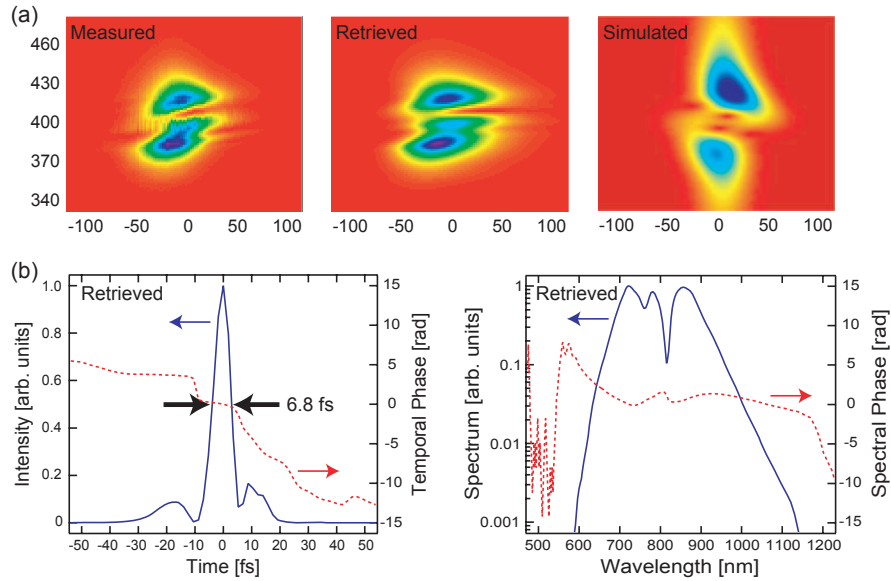


Fig. 7. (a) Measured, retrieved, and simulated XFROG spectrogram of the compressed pulse exiting the nanowire. (b) Retrieved pulse shape and spectrum from the XFROG measurement.

in Fig. 7, and the duration is measured to be 6.8 fs. This corresponds to a compression factor F_c of 10.29 and to a quality factor Q_c of 0.73. The measured spectral phase of the continuum varies only by about 5 rad. The simulated result for this interaction assuming a 57 percent coupling efficiency yields good agreement with experiment and is also shown in Fig. 7. A higher power coupling objective was used for this measurement which accounts for the improved coupling efficiency. This coupled power corresponds to a soliton order of $N = 6.9$.

6. Conclusion

We have shown through simulation and experiment that photonic nanowires with wavelength-sized core diameters and millimeter lengths provide suitable conditions for broadband soliton-effect compression of ultrafast pulses. Compression to single-cycle durations is predicted in simulations using the nonlinear-envelope equation. Compression of a 70-fs input pulse to a 6.8-fs few-cycle duration is experimentally demonstrated using XFROG. Soliton-effect compression in photonic nanowires provides a simple method for self-compression of sub-nJ pulses to few-cycle durations. The simplicity of this method should facilitate investigations of few-cycle pulse propagation and light-matter interactions.

Acknowledgments

We gratefully acknowledge conversations with John M. Dudley. This work was supported by NSF under award number ECS-0200415. M.A.F. and A.L.G. also acknowledge support by the Air Force Office of Scientific Research under contract number F49620-03-1-0223.